Dynamic Spectrum Tracking using Energy and Cyclostationarity-based Multi-variate Non-parametric Quickest Detection For Cognitive Radios

Yang Li, and Sudharman K. Jayaweera, *Senior Member, IEEE*

***Abstract*—A novel non-parametric, multi-variate quickest detection method is proposed for cognitive radios (CRs) using both energy and cyclostationary features. The proposed approach can be used to track state dynamics of communication channels. This capability can be useful for both dynamic spectrum sharing (DSS) and future CRs, as in practice, centralized channel synchronization is unrealistic and the prior information of the statistics of channel usage is, in general, hard to obtain. The proposed multi-variate non-parametric average sample power and cyclostationarity-based quickest detection scheme is shown to achieve better performance compared to traditional energy-based schemes. We also develop a parallel on-line quickest detection/off-line change-point detection algorithm to achieve self-awareness of detection delays and false alarms for future automation. Compared to traditional energy-based quickest detection schemes, the proposed multi-variate non-parametric quickest detection scheme has comparable computational complexity. The simulated performance shows improvements in terms of small detection delays and significantly higher percentage of spectrum utilization.**

***Index Terms*—Cognitive radio, Radiobot, spectrum sensing, cyclostationarity, non-parametric quickest detection.**

I. Introduction

The increasing demand for mobile wireless services, such as web browsing, video telephony, and video streaming, with various constraints on delay and bandwidth requirements, poses new challenges to future generation wireless communication networks. To address the pressing shortage of spectrum to meet these demands, the National Broadband Plan (NBP) [1] from the Federal Communications Commission (FCC) recommends freeing up 500MHz of spectrum for broadband use in the next 10 years with 300MHz being made available for mobile use in the next five years [1]. The plan proposes to achieve this goal in a number of ways: incentive auctions, repacking spectrum, and enabling innovative spectrum access models that take advantage of opportunistic spectrum access (OSA) and cognitive techniques. The plan urges the FCC to initiate further developments on OSA beyond the already completed TV white space allocation. In-line with the above vision, the *Radiobot* architecture proposed in [2]–[7] envisions broadband cognitive radios (CRs) that are not limited to a single radio network. The Radiobot concept aims at future autonomous and self-reconfigurable wide-band CRs, which require both state-of-the-art RF front-end and sophisticated signal processing techniques.

Y. Li and S. K. Jayaweera are with the Department of Electrical and Computer Engineering, University of New Mexico, Albuquerque, NM, USA, Email: {yangli, jayaweera}@ece.unm.edu.

Spectrum awareness is one of the most critical elements of any CR system [2]. Previous work on CRs and dynamic spectrum sharing (DSS) often assumes that the cognitive radio networks (CRNs) are time-slotted (see [8] and references therein). In time-slotted CRNs, the primary users (PUs) become active or idle at the start of a time slot. During one time slot, the PUs state is not changed. Therefore, the secondary users (SUs) can spend a short sensing period at the beginning of each time slot to determine the spectrum availability. At the end of the sensing period, SUs may transmit their data if the inferred spectrum state is idle, otherwise they must remain silent. However, in more general cases, primary networks may not be time-slotted. Even when they are time-slotted, autonomous CRs may not be able to be synchronized with the primary networks. As a result, the PUs may change their states at any time from the point of view of autonomous CRs, and thus the CRNs are non-time-slotted. Performing periodic spectrum sensing is no longer sufficient to keep track of the state changes of the communication channels in non-time-slotted CRNs. Instead, one may have to resort to the quickest detection (QD) methods.

In the QD problem, one observes samples sequentially. Initially, the samples are drawn from a certain distribution. At an unknown time, the distribution changes. Once this occurs, one needs to raise an alarm as quickly as possible to minimize the detection delay [9]. In non-time-slotted CRNs, the on/off radio activities at unknown times will change the distribution of the received signal by a CR. In general, QD schemes can be classified into parametric and non-parametric schemes. Parametric QD schemes rely on the knowledge of the pre-change and post-change distributions of the observations. However, in a variety of applications, including detecting radio activities in an unknown RF environment, such prior knowledge may be hard to obtain due to uncertainties induced by channel fading, channel shadowing, the distance to the primary radios, and Doppler effects, among others. In comparison, a non-parametric QD scheme does not require any knowledge of the pre-change and post-change distributions.

In [10], QD methods were proposed for CRs. Both parametric and non-parametric based algorithms were discussed and analyzed. However, the discussed methods were only

based on energy features. Note that the detection reliability can be compromised by using energy features alone under channel shadowing, since variation of the received signal power level may trigger excessive false alarms. Moreover, the non-parametric approach proposed in [10] uses the individual sample power as the test statistics instead of the average sample power over a certain duration. This, however, significantly increases the number of detection/observation steps leading to a high computational complexity compared to using a time window to obtain the average sample power. In this paper, we show that the choice of the time window length plays a critical role in determining the achieved detection delay, false alarm rate, as well as the percentage of idle channel utilization. Setting the time window length down to one sample is evidently not the best choice.

In [3], the authors developed a blind energy and cyclostationarity-based signal identification and classification procedure that does not rely on any prior knowledge of the radio environment. It is also shown in [3] that the cyclostationarity-based signal features are robust against channel fading, shadowing and Doppler effects. As a result, in this paper, we propose to utilize the cyclostationarity feature to overcome the aforementioned reliability issue of the traditional energy-based QD approach in complex channel conditions, and to exploit diversity to improve the detection performance. To the best of our knowledge, such an average sample power and cyclostationarity-based multi-variate non-parametric QD has not been previously considered in literature. Moreover, the performance of the proposed QD algorithms is evaluated in more realistic multi-path frequency-selective fading channels with Doppler effects, compared to [10].

The main contributions of this paper include: 1) the proposal of the average sample power and cyclostationarity-based multi-variate non-parametric QD strategy for CRs; and 2) the proposal of the parallel on-line QD/off-line change-point detection strategy that is used to provide information of detection delays and false alarm rates as feedback for possible machine learning techniques to achieve future autonomous operation. Note that originally multi-variate non-parametric QD strategy was proposed in [11]. The incorporation of the machine learning techniques to achieve autonomous operation is left as future work due to the focus of this paper and the space limitation. The computational complexities of the energy-based uni-variate non-parametric QD method and the multi-variate non-parametric QD method are also compared in this paper. We show that the multi-variate QD method has a comparable complexity to the uni-variate case, depending on the choice of time window length of each sensing step. The simulation also shows that the proposed multi-variate QD method outperforms the energy-based uni-variate case, in terms of the detection delays and the percentage of idle channel usage.

Note that, the proposed non-parametric QD scheme in this paper can be used for detecting both state transitions from idle to busy, and those from busy to idle. Since the only transmission opportunities for a CR happen when the channel is idle, it is desirable to actually utilize the channel while the QD is in progress detecting a state change from idle to busy. However, this may not be possible when a CR uses traditional half-duplex radio front-ends since they do not support simultaneous transmission and reception of different signals in the same channel. As a result, it is advantageous to consider a possible full-duplex RF front-end in this context. Several full-duplex proposals haven been shown in literature [12]–[15] due to recent advances in radio frequency (RF) front-ends. Although the full-duplex radio front-ends can provide benefits in terms of transmission, the proposed QD method does not depend on the full-duplex radio front-ends and works equally well with traditional half-duplex front-ends. In this paper, full-duplex radio front-ends are not discussed any further. The incorporation is left as a future task.

The remainder of this paper is organized as follows. In Section II we describe our system model. The uni-variate non-parametric QD scheme is then briefly described to prepare the reader for subsequent sections. In Section III, we propose the non-parametric average sample power-based and the cyclostationarity-based QD schemes. We then propose the average sample power and cyclostationarity-based multi-variate non-parametric QD, followed by the novel parallel on-line QD/off-line change-point detection scheme. In Section IV we present performance evaluation of the proposed QD schemes through simulations. In Section V we conclude by summarizing our results and identifying possible future directions.

II. System Model and Non-parametric Quickest Detection

Due to the focus of this paper on the QD algorithm, we consider the spectrum sensing for a particular communication channel and omit the decision-making problem for scheduling of which channel to sense at any given time. Note that the proposed methods in this paper work for detecting the state transitions from either idle to busy or from busy to idle. Without loss of generality, first we may consider the case of detecting a change from idle to busy. The detection of changes from busy to idle is further explained in later sections. We assume that after a state change is detected, observations corresponding to the past are discarded. Thus, a new observation vector is obtained by re-initializing the starting point as the previous detection point. As a result, by applying the proposed method iteratively, we may detect each state change-point in a sequence of multiple alternating state change cycles, as long as those changes are sufficiently far apart in order to obtain enough observation data to make a decision. Hence, for the proposed QD schemes to work properly, we assume that the sampling rate is set at a higher rate compared to the rate of state changes. For example, in the simulation section, we assume that the minimum sojourn times of idle and busy channel states are 600μS (a reasonable assumption according to [16]), while sensing sampling rate is 100MHz. For a certain communication channel of interest, we denote by vector $\mathbf{Z}_1^n = [Z_1, Z_2, \cdots, Z_n]^T$ the sequence of observations or test statistics from time step 1 up to n, depending on the adopted particular sensing technique, including for example, energy detection and cyclostationarity-based detection, etc. At

each time n, a CR attempts to distinguish the following two hypotheses based on $\mathbf{Z}_1^n$:

$$\begin{aligned} \mathcal{H}_0: &\quad Z_i \sim g_0,\ \forall\ i \in \{1, \cdots, n\} \\ \mathcal{H}_1: &\quad \exists\ \tau \in \{1, \cdots, n\}, \\ &\quad \text{s.t.} \begin{cases} Z_i \sim g_0, \forall\ i \in \{1, \cdots, \tau - 1\} \\ Z_i \sim g_1, \forall\ i \in \{\tau, \cdots, n\} \end{cases}, \end{aligned} \quad (1)$$

where we denote by g_0 and g_1, respectively, the distribution of Z_i under channel idle and busy hypotheses and τ denotes the time of the state change from idle to busy. We denote by Γ the strategy adopted for the hypothesis testing and denote by t_a the time when the strategy raises an alarm of a state change. If $t_a \geq \tau$, the detection delay is defined as $\tau_d = t_a - \tau$. On the other hand, if $t_a < \tau$, we say a false alarm occurs. Due to the fact that a prior distribution for the change point is generally hard to find and the statistics of the state change pattern can easily be non-stationary, we consider the QD in a non-Bayesian framework.

Note that the channel allocation information[1] can generally be unknown to a Radiobot *a priori*. However, by following the procedure of the RF activity detection and classification introduced in [3], one may classify the RF activities according to their center frequencies, cyclostationary features (symbol duration, coding structures, etc.), and bandwidths to obtain the knowledge of the RF spectrum usage, so that channel allocation information can be inferred and identified within the frequency range of interest.

In the framework of non-Bayesian QD, the *worst case conditional mean delay* is usually defined as [9], [17]

$$\bar{T}_d = \sup_{\tau \geq 1} \operatorname{ess\,sup} \mathbb{E}_{g_1}\{\tau_d = t_a - \tau \mid t_a \geq \tau, \mathbf{Z}_1^\tau\}, \quad (2)$$

where $\mathbb{E}_{g_1}\{\cdot\}$ denotes expectation under the distribution g_1, and the operator $\operatorname{ess\,sup}$ denotes the essential supremum or the smallest essential upper-bound. The conditioning within the expectation is with respect to the change point, and the worst case is taken over all possible values of the change point and all realizations of the measurements or the obtained test statistic sequence up to the change point. Note that the conditional mean delay can be defined as $\mathbb{E}_{g_1}\{\tau_d = t_a - \tau \mid t_a \geq \tau, \mathbf{Z}_1^\tau\}$ [9], which itself is random since τ and $\mathbf{Z}_1^\tau$ are random. One could assign a prior distribution to τ, and then define average delay by averaging the distribution on τ and $\mathbf{Z}_1^\tau$. However, it may be difficult to find a suitable prior distribution for τ in the application of cognitive radios. As a result, the worst case, meaning using the least favorite distributions of τ and $\mathbf{Z}_1^\tau$, is considered by taking the essential supremum over $\mathbf{Z}_1^\tau$, and taking the supremum over τ to the conditional mean delay. We may also define the average run length (ARL) to false alarm (mean value of the false alarm intervals) to be

$$\bar{T}_f = \mathbb{E}_{g_0}\{t_a\}, \quad (3)$$

[1]Within the frequency range covered by each configuration of the reconfigurable antenna, there can, in general, be multiple channels belonging to possibly different systems, according to a static RF spectrum allocation scheme. The allocated channels generally may have different center frequencies as well as their bandwidths.

where $\mathbb{E}_{g_0}\{\cdot\}$ denotes expectation under the distribution g_0. Note that in (3), the condition $t_a < \tau$ is not included since it is redundant. On the other hand, no essential supremum is taken, so the condition on $\mathbf{Z}_i$'s is also not necessary.

The optimization problem can then be defined to find the strategy Γ that minimizes $\bar{T}_d$ while satisfying a lower threshold T_{th} for the ARL to false alarm $\bar{T}_f$:

$$\begin{aligned} \min_{\Gamma} \quad & \bar{T}_d = \sup_{\tau \geq 1} \operatorname{ess\,sup} \mathbb{E}_{g_1}\{\tau_d = t_a - \tau \mid t_a \geq \tau, \mathbf{Z}_1^\tau\}, \\ & \text{subject to } \bar{T}_f \geq T_{th}. \end{aligned} \quad (4)$$

Let us denote by G_0 and G_1 respectively the cumulative distribution functions (cdfs) of Z_i corresponding to g_0 and g_1, such that $G_0(z) = \int_{-\infty}^{z} g_0(x)dx$ and $G_1(z) = \int_{-\infty}^{z} g_1(x)dx$. Note that G_1 is said to be stochastically greater [18] than G_0 when $G_0(x) \geq G_1(x)$ for all x, and we can write $G_1 \succ_{st} G_0$.

Observe that if for a particular random process Z_i, for $i = 1, 2, 3, \cdots$ such that the cdfs $G_{Z,0}$ and $G_{Z,1}$ instead satisfy $G_{Z,0} \succ_{st} G_{Z,1}$, and if we denote by $X_i = -Z_i$ another process with corresponding pre-change and post-change cdfs denoted by $G_{X,0}$ and $G_{X,1}$, then it is straightforward to show that $G_{X,1} \succ_{st} G_{X,0}$. This makes it easy to adopt the same QD algorithm explained in the following for both detecting the state changes from idle to busy and those from busy to idle. In case of detecting the state changes from busy to idle, we may simply add a negative sign in front of the obtained test statistics Z_i's such that the post-change distribution is stochastically greater then the pre-change distribution.

From the observation vector $\mathbf{Z_1^n} = [Z_1, \cdots, Z_n]$, we may define the rank for the i-th observation Z_i, as $\rho(i, n) = \sum_{j=1}^{n} I_{\{Z_i \geq Z_j\}}$, where $I_{\{E\}}$ is the indicator function of event E, defined as $I_{\{E\}} = 1$ if event E is true and $I_{\{E\}} = 0$ otherwise. Thus, a higher valued observation Z_i has a higher rank $\rho(i, n)$ in the first n observations. Then, we may take $\boldsymbol{\rho}_n = [\rho(1, n), \cdots \rho(n, n)]$ to determine a permutation of the first n integers. Its inverse permutation can be determined as $\boldsymbol{\mu}_n = [\mu(1, n), \cdots, \mu(n, n)]$, where we define $\mu(\rho(j, n), n) = j$, such that the function $\mu(\rho(j, n), n)$ returns the time sequence index j of an observation with rank $\rho(j, n)$.

With these definitions, the likelihood ratio of the change taking place at $\tau = k$, for $k \in \{1, \cdots, n\}$, and observing a particular $\boldsymbol{\rho}_n$ is given by

$$\Lambda_k^n(\boldsymbol{\rho}_n) = \frac{P\{Z_{\mu(1,n)} < \cdots < Z_{\mu(n,n)} \mid \tau = k\}}{P\{Z_{\mu(1,n)} < \cdots < Z_{\mu(n,n)} \mid \tau > n\}}. \quad (5)$$

Since the above rank based likelihood ratio is not too sensitive to the true underlying distributions [18], one can compute this likelihood ratio by choosing some representative/hypothesized pre and post-change distributions and design a corresponding algorithm based on this likelihood ratio [18]. Note that the invariance of the ranks under strictly increasing transformations causes the average run length (ARL) to false alarm to be identical for any continuous G_0.

For example, if we choose the representative/hypothesized pre and post-change pdfs as $f_0(x) = e^{-|x|}/2$ and $f_1(x) = p\alpha e^{-\alpha x} I_{\{x \geq 0\}} + q\beta e^{\beta x} I_{\{x < 0\}}$, with $p \in (1/2, 1)$, $\alpha \in (0, 1)$, $\beta \in [1, +\infty)$, and $q = 1 - p$ [18], then we have the following

cdfs:

$$F_0(x) = \begin{cases} \frac{1}{2}e^{x}, & \text{if } x < 0 \\ 1 - \frac{1}{2}e^{-x}, & \text{if } x \geq 0 \end{cases}, \tag{6}$$

$$F_1(x) = \begin{cases} qe^{\beta x}, & \text{if } x < 0 \\ 1 - pe^{-\alpha x}, & \text{if } x \geq 0 \end{cases}. \tag{7}$$

If we make $p\alpha \geq q\beta$, then we can verify that the F_1 is stochastically greater than F_0.

According to [18], the likelihood ratio function in this case can then be expressed as

$$\Lambda_k^n(\boldsymbol{\rho}_n) = \sum_{i=0}^{n} \lambda_{k,i}^n(\boldsymbol{\rho}_n), \tag{8}$$

where

$$\begin{aligned} \sum_{m=0}^{n} \lambda_{k,m}^n(\rho_n) &= \binom{n}{m}\left(\frac{1}{2}\right)^n \left(\frac{p\alpha}{q\beta}\right)^{U_k(m,n)} (2q\beta)^{n+1-k} \\ &\times \prod_{i=1}^{m}\left(1 + \frac{V_k(i,n)}{i}(\beta - 1)\right)^{-1} \\ &\times \prod_{i=m+1}^{n}\left(1 + \frac{U_k(i-1,n)}{n+1-i}(\alpha - 1)\right)^{-1}, \end{aligned} \tag{9}$$

with $U_k(m,n) = \sum_{j=k}^{n} I_{\{\rho(j,n) > m\}}$, and $V_k(m,n) = (n + 1 - k) - U_k(m,n)$ [18].

The procedure for the QD provided in [18] is to compute the Shiryayev-Roberts statistic $R_n = \sum_{k=1}^{n} \Lambda_k^n(\boldsymbol{\rho}_n)$ and to stop at time t_a when R_n first achieves or exceeds the critical level A. The ARL to false alarm is shown in [18] to be lower-bounded as

$$A \leq \mathbb{E}_{g_0}\{t_a\}, \tag{10}$$

and the ARL to false alarm is shown to grow asymptotically linearly in A as the critical level becomes large. The detection delay is shown in [18] to be upper-bounded as

$$\limsup_{A\to\infty} \sup_{\tau \geq \tau(A)} \mathbb{E}_{g_1}\{t_a - \tau \mid t_a \geq \tau\} \leq \frac{\log(A)}{D(G_0, G_1; f_0, f_1)}, \tag{11}$$

where

$$D(G_0, G_1; f_0, f_1) = \mathbb{E}_1\left\{\log\left(\frac{f_1(F_0^{-1}(G_0(Z_1)))}{f_0(F_0^{-1}(G_0(Z_1)))}\right)\right\}. \tag{12}$$

The computational complexity of this uni-variate non-parametric QD procedure can be shown to be $\mathcal{O}(n^4)$ [18].

III. Average Sample Power and Cyclostationarity-based Multi-variate Non-parametric Quickest Detection

A. Non-parametric Average Sample Power-based Quickest Detection Scheme

When there is no prior information about the signal of interest, at any time instance one may model the received signal in a particular channel as $Y = W$ under the assumption of no communication activity, where we denote by W the noise; and $Y = X + W$ when communication activities are present, where we denote by X the received signal contributed from the activity. When the distributions of Y under both activity absent and present are hard to find, or the distribution parameters are unknown, one may adopt the above introduced uni-variate non-parametric QD. The authors in [10] proposed to use the sample powers as the test statistic Z_i's in the non-parametric change-point detection method discussed above, which has a computational complexity of $\mathcal{O}(n^4)$. However, we find that this method is unsuitable when the idle/busy periods last for a length that is at least several transmission-packets long, which is normally the case. This is because the computational complexity becomes high when the size of the vector $\mathbf{Z}_1^n$ is large. Instead, in this paper, we propose to use a number of consecutive samples to compute an average signal power as the test statistic. In particular, we assume that for every M number of samples, we compute $Z_i = \frac{1}{M}\sum_{j=1+(i-1)M}^{iM} |Y(j)|^2$ as the test statistic. In this case, the computational complexity of obtaining the average power at each step is $\mathcal{O}(M)$. Thus, the computational complexity of the overall uni-variate non-parametric QD scheme becomes $\mathcal{O}(Mn^4)$. It is straightforward to see that, by increasing the number of samples M in each step, the expected number of detection steps n may be significantly reduced. As a result, a lower computational complexity may be obtained by using a time window to compute an average power, instead of using individual sample powers for the QD. In the simulations section, we also investigate the effect of the choice of M in terms of the detection delays and false alarm rates. In this case, the ARL to false alarm and the detection delay are as characterized in (10) and (11), respectively.

B. Non-parametric Cyclostationarity-based Quickest Detection Scheme

It is well-known that almost all man-made signals exhibit some underlying periodicities due to, for example, their symbol rates, coding schemes, packet/frame header structures and training symbol sequences, etc. [19]. We consider a cyclostationary digital signal $x(t)$ and a general linear time-varying (LTV) fading channel[2] having an impulse response of $h(\tau', t)$. From the definition of cyclostationarity, the auto-correlation function of $x(t)$ is a periodic function of t, i.e. $R_{xx}(t + T_0, \tau) = R_{xx}(t, \tau)$, for some period T_0. The received signal $y(t)$ through the LTV fading channel can be expressed as:

$$y(t) = \int_0^{\infty} x(t - \tau')h(\tau', t)d\tau' + w(t), \tag{13}$$

where $w(t)$ is an additive wide sense stationary (WSS) noise process. Under the assumption of the channel being wide sense stationary and uncorrelated scattering (WSSUS)[3] which

[2]Time-varying is due to relative motion between the transmitter and receiver. Note that the LTV channels are also referred to as time-frequency dispersive/selective or doubly dispersive/selective in the literature.

[3]According to empirical studies, the channel can be considered as WSS as long as the mobile unit (the transmitter and/or receiver) covers a distance in the order of a few tens of the wavelength of the carrier signal during an observation period [20]. We also assume that scattering components with different propagation delays are statistically uncorrelated. These channel models are called US (uncorrelated scattering) channel models or US models [21]. The most important class of stochastic LTV channel models is represented by models belonging both to the class of WSS and to the class of US.

is almost exclusively employed in literature for modeling frequency selective mobile radio channels [20]–[24], it has been shown in [3] that the autocorrelation function of the received signal $y(t)$ is also periodic with the same period T_0 as the transmitted signal $x(t)$, so that the received signal $y(t)$ is also cyclostationary with the same cyclic components as $x(t)$.

Using the discrete-frequency smoothing method [19] described below, we may compute an estimate of the Spectral Correlation Function (SCF) $S_x^\alpha(t,f)$ for a general discrete signal $\{x(t-kT_s)\}_{k=0}^{M-1}$ in a particular channel (assuming that the signal is band-limited to the frequency range from f_L to f_H), with M number of samples and a sampling period of T_s. The FFT $\tilde{X}(t,f)$ of the sequence $\{x(t-kT_s)\}_{k=0}^{M-1}$ is defined in (14) over the set of frequencies $\{-\frac{f_s}{2}, -\frac{f_s}{2}+F_s, \cdots, \frac{f_s}{2}-F_s, \frac{f_s}{2}\}$, where $f_s = \frac{1}{T_s}$ is the sampling rate and $F_s = \frac{1}{MT_s}$ is the frequency increment and $a(t)$ is a triangular data tapering window [19].

$$\tilde{X}(t,f) = \sum_{k=0}^{M-1} a(t-kT_s)x(t-kT_s)e^{-j2\pi f(t-kT_s)}. \quad (14)$$

An estimate of the SCF can then be obtained [19] based on the discrete-frequency smoothing method:

$$\tilde{S}_x^\alpha(t,f) = \frac{1}{LT}\sum_{\nu=-(L-1)/2}^{(L-1)/2} \tilde{X}(t, f+\frac{\alpha}{2}+\nu F_s)\tilde{X}^*(t, f-\frac{\alpha}{2}+\nu F_s),$$

where $T = MT_s$ is the time length of the data segment, α is the cyclic frequency and L (an odd number) is the spectral smoothing window length. An estimate of the spectral autocoherence function magnitude [19] can then be computed as:

$$|\tilde{C}_x^\alpha(t,f)| = \frac{|\tilde{S}_x^\alpha(t,f)|}{\sqrt{\tilde{S}_x^0(t,f+\alpha/2)\tilde{S}_x^0(t,f-\alpha/2)}}, \quad (15)$$

for all $f \in [f_L, f_H]$. Note that $|\tilde{C}_x^\alpha(t,f)|$ is normalized to be between 0 and 1. A *channel cyclic profile* for a channel from f_L to f_H can then be defined as

$$\tilde{I}_x(t,\alpha) = \max_{f\in[f_L,f_H]} |\tilde{C}_x^\alpha(t,f)|. \quad (16)$$

The authors in [3] proposed a blind cyclostationarity-based signal identification and classification strategy, which extracts the underlying cyclic components induced by their symbol rates and coding structures *without any prior information*. The cyclic components induced by signal symbol rates and coding structure can be extracted by finding local maxima of $\tilde{I}_x(t,\alpha)$. The local maxima are not hard to be determined by setting a threshold to the cyclic profile since the profile has sharp peaks at the cyclic frequencies corresponding to the symbol rate and coding rate. The same authors in [3] also developed a machine learning based algorithm for setting the threshold of the cyclic profile in order to better extract the cyclic components without any prior information in a later work in [7]. Due to the space limitation and the focus of this work, we do not present more details of this blind cyclostationarity-based signal identification and classification procedure in this paper. By utilizing the blind signal identification and classification method in [3], we may obtain knowledge of the channel information including channel carrier frequency, bandwidth, and cyclic components associated with each channel. On the other hand, in the context of traditional dynamic spectrum sharing, channel information and primary signal characteristics, such as carrier frequency, signal bandwidth, symbol rates etc., are generally assumed to be known beforehand. As a result, the following proposed QD schemes are applicable for the traditional CRs as well.

Assuming a particular cyclic frequency α_0 that is of interest for a particular channel from f_L to f_H, one may compute the value of $\tilde{I}_x(t,\alpha_0)$. It can be seen from (15) and (16) that, $\tilde{I}_x(t,\alpha_0)$ takes value in the interval of $(0,1)$. However, due to channel fading, shadowing effects, sensing duration, sampling frequency, unknown signal-to-noise ratio (SNR), and estimation errors etc., the distribution of $\tilde{I}_x(t,\alpha_0)$ is generally hard to find in closed-form. As a result, in this paper we propose to use the non-parametric scheme as introduced in [18] to perform the QD. We assume that for every M time samples of the received signal of interest, at a sampling rate of f_s, we may obtain a test statistic $Z_i = \tilde{I}_x(i,\alpha_0)$, in which we replaced the time index t by the sequence index i to indicate the i-th test statistic. We denote by G_0 and G_1 the cdf of Z_i under hypothesis $\mathcal{H}_0$ and $\mathcal{H}_1$, respectively. It has been shown in [3] that when an RF signal with the cyclic component α_0 is present, the function $\tilde{I}_x(i,\alpha)$ tends to exhibit a local peak with a value close to 1 at $\alpha = \alpha_0$; and on the other hand, if the signal is absent, the function tends to have a low value close to 0 at $\alpha = \alpha_0$. Consequently, it is reasonable to assume that the distribution G_1 is stochastically greater than G_0 and we verify this by simulations in the following.

As shown in Fig. 1, we obtained the estimated cdfs of the averaged sample power and $\tilde{I}_x(i,\alpha_0)$ at $\alpha_0 = 1$MHz under both signal absent and present scenarios (we plot the cdfs of the average sample power in Fig. 1 in order to compare to the cyclostationarity-based case) with various sensing time window lengths and three different SNRs: -10dB, 0dB and 5dB. The simulated signal is a Bluetooth signal with a symbol duration of 1μS (i.e., a resulting symbol rate cyclic frequency feature at 1MHz). The channel is a frequency-selective (multi-path) fading channel with a maximum Doppler shift of $\pm$300Hz, which corresponds to a maximum transmitter-receiver relative speed of 37.5m/s, or around 84 mph for a signal in the 2.4GHz frequency range. There are three discrete paths specified with their delays 0μS, $.15\mu$S, and $.32\mu$S, respectively, and with an average path gain of 0dB, -10dB, and -10dB, respectively. Each discrete path is modeled as an independent Rayleigh fading process. As is seen from Fig. 1, in all cases, the resulting G_1 (signal present) is stochastically greater than G_0 (signal absent), or $G_1 \succ_{st} G_0$.

We can also see from Fig. 1 that when the SNR is low (-10dB), the pre and post-change cdfs of the averaged sample power does not differ as much compared to the case of $\tilde{I}_x(i,\alpha_0)$, even with a long sensing time (200μS). On the contrary, the pre and post-change cdfs of $\tilde{I}_x(i,\alpha_0)$ differ from each other noticeably even when $SNR = -10$dB with a sensing time of 100μS. Intuitively, the more the pre- and post-change cdfs are distinguishable, the better detection perfor-

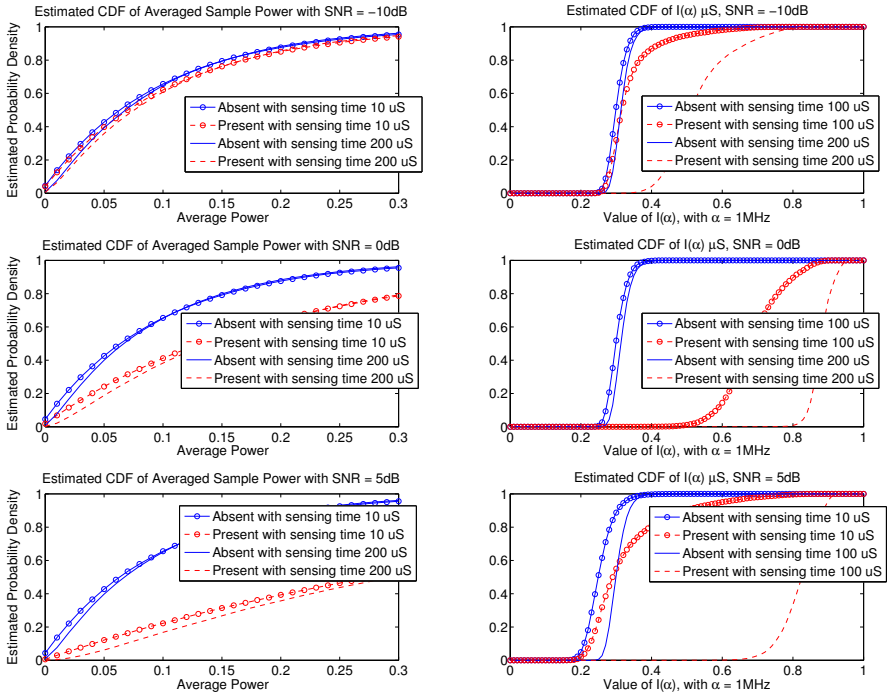

Fig. 1. Estimated cdfs for the averaged power and $\tilde{I}_x(t, \alpha_0)$ when the signal with cyclic component α_0 is absent and present.

mance can be expected in terms of the averaged detection delay and ARL to false alarms. This suggests that when the SNR is low, the cyclostationarity-based scheme can be more effective with longer sensing time window length. On the other hand, as we can see from Fig. 1, with a short sensing time of 10μS at $SNR = 5$dB, the difference between the pre- and post-change cdfs is greater in the case of the averaged sample power, compared to the difference of those of $\tilde{I}_x(i, \alpha_0)$. This suggests that, when SNR is high, the average sample power-based QD scheme may be more efficient. This is because a short sensing time for the cyclostationarity-based case is not adequate for obtaining distinguishable pre- and post-change cdfs as in the average sample power-based case. It is then straightforward to see that the sensing time length can be a critical factor of the efficiency and the effectiveness of the QD. In particular, by using a longer sensing time length in both cases, more distinguishable pre- and post-change distributions are obtained for the metrics. However, note that the detection delay is expressed in terms of the observation steps in [18] as discussed in Section II. Thus, the detection delay of the proposed non-parametric QD method in this paper is given by the product of the number of observation steps and the sensing time length at each step. As a result, a longer sensing time length setting for each observation step may also increase the overall detection delay.

From the above observations, it is reasonable to exploit the diversity and consider combining the energy-based and the cyclostationarity-based QD schemes, since each offers distinct advantages and disadvantages under different conditions. In particular, one may consider a vector test statistic based on the observations of the averaged sample power and the value of $\tilde{I}_x(i, \alpha_0)$ for each operation step, and perform the QD. In the next sub-section, we discuss such a multi-variate QD scheme.

C. Average Sample Power and Cyclostationarity-based multi-variate Quickest Detection

Combining the average sample power-based and the cyclostationarity-based test statistics at each time step, we may generate a multi-variate observation at each step by stacking the obtained average sample power and $\tilde{I}_x(i, \alpha)$ into a 2×1 column vector at each time, i.e. at time n, with a slight abuse of the notation, we obtain the matrix

$$\mathbf{Z}_1^n = [\mathbf{Z}_1 \mathbf{Z}_2, \cdots, \mathbf{Z}_n], \tag{17}$$

where we denote by $\mathbf{Z}_i$'s 2×1 column vectors, for all $1 \leq i \leq n$. In [25], a class of multivariate rank-like quantities is defined and used to develop multivariate tests to mimic traditional one-dimensional rank tests. We may adopt the algorithm developed in [11] to define the centered directional rank vector [11] of $\mathbf{Z}_i$ for all $1 \leq i \leq n$ as

$$\mathbf{R}_n(\mathbf{Z}_i) = \sum_{j=1}^{n} \mathbf{D}_{ij}, \tag{18}$$

where we let

$$\mathbf{D}_{ij} = \frac{\mathbf{Z}_i - \mathbf{Z}_j}{||\mathbf{Z}_i - \mathbf{Z}_j||}. \tag{19}$$

The interpretation is that $\mathbf{D}_{ij}$ is a unit vector pointing from $\mathbf{Z}_j$ to $\mathbf{Z}_i$, or the normalized difference between $\mathbf{Z}_i$ and $\mathbf{Z}_j$. The centered directional rank vector $\mathbf{R}_n(\mathbf{Z}_i)$ may be considered as

the accumulated difference between the point $\mathbf{Z}_i$ and the rest of data points, similar to the idea of ranking in the traditional one-dimensional case. We may then define the test statistic $R_{k,n}$ as

$$R_{k,n} = \bar{\mathbf{R}}_n^{(k)^T} \hat{\mathbf{\Sigma}}_{R_{k,n}}^{-1} \bar{\mathbf{R}}_n^{(k)}, \tag{20}$$

where

$$\bar{\mathbf{R}}_n^{(k)} = \frac{1}{k} \sum_{i=1}^{k} \mathbf{R}_n(\mathbf{Z}_i), \tag{21}$$

and

$$\hat{\mathbf{\Sigma}}_{R_{k,n}} = \frac{n-k}{(n-1)nk} \sum_{i=1}^{n} \mathbf{R}_n(\mathbf{Z}_i) \mathbf{R}_n(\mathbf{Z}_i)^T, \tag{22}$$

for $k = 1, \cdots, n$. Note that $\bar{\mathbf{R}}_n^{(k)}$ may be interpreted as the average of the first k ranking values. If $\{\mathbf{Z}_1 \cdots \mathbf{Z}_k\}$ are from the same distribution, then these data points are located more closely compared to the case in which there exists a distribution change before the k-th point. As a result, comparatively, a shorter vector $\bar{\mathbf{R}}_n^{(k)}$ is obtained for the case of no distribution change, and a longer vector $\bar{\mathbf{R}}_n^{(k)}$ is obtained for the case with a distribution change before the k-th point. Then, the quadratic term $R_{k,n}$ of $\bar{\mathbf{R}}_n^{(k)}$ may be used as the test statistic to detect a distribution change point, since $R_{k,n}$ reflects the length of the vector $\bar{\mathbf{R}}_n^{(k)}$, which is affected by the existence/absence of a change point. The QD may then proceed as follows: 1) obtain $R_{max,n} = \max_{1<k\leq n} R_{k,n}$; 2) If $R_{max,n} > h_{n,p_f}$, raise an alarm for state change, otherwise collect another multi-variate vector observation and repeat steps 1) and 2). The threshold h_{n,p_f} is chosen such that the conditional probability of a false alarm when observation n is added is equal to p_f, given that no previous false alarm has occurred, or

$$\Pr\{R_{max,n} > h_{n,p_f} \mid R_{max,j} \leq h_{j,p_f}; j < n\} = p_f. \tag{23}$$

Note that again this detection method works for both detecting the state changes from idle to busy as well as for detecting those from busy to idle. However, as also noted in [11], finding an analytical solution for the sequence of control thresholds h_{n,p_f} is generally difficult due to the unknown distributions of the observations in the first place. As a result, we resort to simulations in Section IV to illustrate the performance of this combined QD scheme. In practice, we suggest to combine this approach with a suitable machine learning (adaptive) technique [26] to obtain the appropriate control thresholds. However, this is out of the scope of this paper and left as a future research task.

The computational complexity of the proposed multi-variate non-parametric QD algorithm can be shown to be linear in n^3, i.e. $\mathcal{O}(n^3)$, where n denotes the number of time steps before a state-change detection. However, the author in [11] has developed a recursive algorithm to make the computational complexity of the multi-variate QD algorithm linear in n, or $\mathcal{O}(n)$. This is accomplished by deriving an expression to compute the test statistics $R_{k,n+1}$ from $R_{k,n}$. Note that the computational complexity of obtaining average sample power in each step is $\mathcal{O}(M)$, where M denotes the number of samples in each step. Whereas, the computational complexity of obtaining the cyclostationary feature for a particular cyclic frequency in each step is dominated by the fast Fourier transform (FFT), which is $\mathcal{O}(M \log M)$. The overall computational complexity of the proposed multi-variate QD procedure is then $\mathcal{O}(nM \log M)$. On the other hand, the computational complexity of the energy-based uni-variate QD algorithm has a complexity of $\mathcal{O}(Mn^4)$. Thus, when $\log M < n^3$, the complexity of multi-variate case may be expected to be even less than the uni-variate case, due to the recursive algorithm proposed in [11]. In case when M is large and $M \gg n$, the complexities of these two cases should still be comparable.

In our case, since we are dealing with alternating idle and busy state changes, we propose that whenever a state change has been detected, we use new observations after each detection point for the QD of subsequent state changes. In this way, we may control the computation complexity of the proposed multi-variate QD to be manageable. In case of either an idle or a busy state lasts for a long time of period, we may adopt a moving time window to discard older observations and make use of only the recent observations to perform the QD and effectively keep the computation complexity low.

To provide the self-awareness of false alarms and the achieved detection delays in the QD procedure, in the following we propose a novel approach to combine the above QD procedure with an offline change-point detection algorithm.

Whenever a false alarm is encountered, either an alarm of state changing from busy to idle is raised before its actual change, or an alarm of state changing from idle to busy is raised while the state is still idle. In the first case, if the CR (or the Radiobot) further decides to start transmitting data on the monitored channel, collisions with other radio activities may occur. In the second case, though there may not be collisions, valuable spectrum opportunities are lost. In either case, any false alarm can certainly affect the performance of the subsequent QDs, causing detection delays and possibly more subsequent false alarms, since the observations from different distributions (pre-change and post-change) are treated as from the same distribution. Note that, detection delays may also affect the detection performance of subsequent detections in a similar way since a detection delay may omit one or more state alternating cycles (a state change from busy to idle followed by a change back to busy is referred as an alternating cycle and vice versa). In order to provide the self-awareness of false alarms and detection delays to improve subsequent detections, we propose to incorporate a parallel offline change-point detection algorithm with our proposed multi-variate QD algorithm. Although the method of the offline change-point detection has already been discussed in [11], the concept of the combination of QD and the offline change-point detection has not been considered in the literature.

The exact off-line change-point detection procedure can be explained as follows. For a given sequence of observations with a length of N, one may obtain the test statistics

$$R_{k,N} = \bar{\mathbf{R}}_N^{(k)^T} \hat{\mathbf{\Sigma}}_{R_{k,N}}^{-1} \bar{\mathbf{R}}_N^{(k)}, \text{ for all } k = 1, \cdots, N, \tag{24}$$

similarly to the QD procedure described above. Then an

estimate of the change point can be obtained as [11]

$$\hat{\tau}_C = \underset{1\le k\le N}{\arg\max}\ R_{k,N}. \tag{25}$$

The parallel on-line QD/off-line change-point detection algorithm can be explained as follows: The off-line change-point detection procedure is invoked whenever a state change alarm is raised from the on-line QD procedure. The QD outcome is trusted for the time being, so that the QD may drop previous observations, re-initialize and take new observations for a subsequent detection of state change. However, the dropped observations from the previous QD procedure are kept for the off-line change-point detection procedure. As the on-line QD procedure continues, newly obtained observations are also fed into the off-line change-point detection procedure. For a short period of time, the off-line change-point detection algorithm may then re-estimate the past state change-point based on both the newly obtained observations and the kept observation history. If the re-estimated change-point were to be different from the initial result declared by the on-line QD procedure, then the re-estimated change-point from the off-line detector is used to re-initialize the starting point for the current on-line QD procedure. In this way, detection delays are made known to CR by comparing the results from the on-line QD procedure and that from the off-line change-point detection procedure.

On the other hand, in order to detect false alarms, we propose to use an off-line threshold h_{off} on the test statistics: if $\max R_{k,N} \ge h_{off}$, then $\hat{\tau}_C = \underset{1\le k\le N}{\arg\max}\ R_{k,N}$ is used to update the change-point as introduced above; if $\max R_{k,N} < h_{off}$, cancel the state-change alarm and re-initialize the current on-line QD procedure from the previous confirmed state change-point. Note that false alarm rates can be reduced by directly setting a higher threshold in the on-line QD procedure. However, this causes longer detection delays. As an alternative, by having a higher threshold h_{off} for the off-line change-point detection procedure (compared to that of the on-line QD procedure), false alarms can be corrected to some extent without compromising the detection delay performance. Note that since the off-line change-point detection procedure relies on more observations, it can provide more accurate/reliable results on average compared to those obtained in the on-line QD procedure. The detailed procedure of the parallel on-line QD/offline change-point detection is presented in Algorithm 1.

Algorithm 1 Parallel Quickest detection and Offline Change-point detection

Initialization: Alarm flag $f \leftarrow 0$, set offline window wait length c, set threshold h and h_{off}, set $n_p = n_0 = 1$
for $n = 1, 2, 3, \cdots$ **do**
  Obtain observations $\mathbf{Z}_{n_0}^n$
  $R_{k,n} \leftarrow \bar{\mathbf{R}}_n^{(k)^T} \hat{\mathbf{\Sigma}}_{R_{k,n}}^{-1} \bar{\mathbf{R}}_n^{(k)}$, for all $k = n_0, \cdots, n$
  if $\max_{n_0\le k\le n} R_{k,n} \ge h$ **then**
    Set the alarm flag to current step: $f \leftarrow n$
    Keep track of the previous state change-point: $n_p \leftarrow n_0$
    Set current state change point: $n_0 \leftarrow n$
  end if
  if $n = f + c$ and $n \ne c$ **then**
    if $\max_{n_p\le k\le n} R_{k,n} \ge h_{off}$ **then**
      $\hat{\tau}_C \leftarrow \underset{n_p\le k\le n}{\arg\max}\ R_{k,n}$
      Re-initialize starting point as $n_0 \leftarrow \hat{\tau}_C$
    else
      Re-initialize starting point as $n_0 \leftarrow n_p$
    end if
  end if
end for

IV. Simulations and Results

In this section, we show representative simulation results to illustrate the advantages of the proposed methods for the channel state QD in CRs such as Radiobots. Note that all the following simulations are based on the same multi-path frequency-selective channel with Doppler effect as used in Section III-B.

In Fig. 2, a typical situation of the non-parametric cyclostationarity-based (univariate, without using the average sample power) QD procedure introduced in Section III-B is shown. In the top panel, we show the values of $Z_i = \tilde{I}_x(i, \alpha_0)$ up to roughly 15000μS. In the middle panel, the sequentially obtained Shiryayev-Roberts statistic is shown. The QD threshold A for the Shiryayev-Roberts statistic is set to 500. Other parameters are shown in the panel itself. In the bottom panel, the true state change history and the detection results are superposed to show detection delays. The procedure for the average sample power based QD introduced in Section III-A is similar.

Fig. 3 shows a typical scenario of the proposed parallel QD/offline change-point detection procedure. We set the threshold $h_{n,p_f} = 11$ for all n of the on-line QD and $h_{off} = 15$ for the off-line change-point detection. We show the state change history and the QD results in the top panel. In the middle panel, we show the plot of test sequence $R_{k,n}$ for each time an alarm is raised, i.e. when $R_{max,n} > h_{n,p_f}$ where $R_{max,n} = \max R_{k,n}$. In the bottom panel, we show the plot of $R_{k,n}$ for each time the off-line change-point detection is engaged. Note that the off-line change-point detection detects the false alarm ($R_{max,n} < h_{off}$) at stage 1 and detects detection delays from stage 2 to stage 5. The estimated chant-points are re-adjusted for all stages. As shown in the middle panel, the re-adjusted change-point of each stage is the first data point of $R_{k,n}$ sequence of the next stage, which is the same as the maximum point of $R_{k,n}$ of the corresponding stage in the bottom panel. However, the on-line QD point of each stage is the last data point of of $R_{k,n}$ sequence of that stage, as shown in the middle panel. The off-line re-adjusted change-points are closer to the real change-points compared to the on-line estimates.

Fig. 4 shows performance comparisons of the average sample power-based, the cyclostationarity-based, and the multivariate parallel QD strategies. The comparison of average detection delay is shown in Fig. 4(a), the probability of

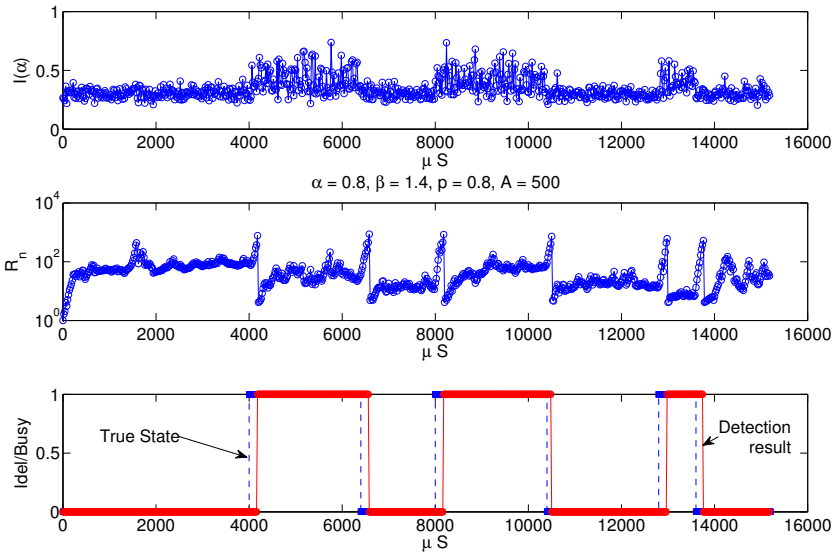

Fig. 2. A typical scenario of the QD procedure at $SNR = 0$dB, with a sampling rate at 100MHz and the sensing time interval of 20μS.

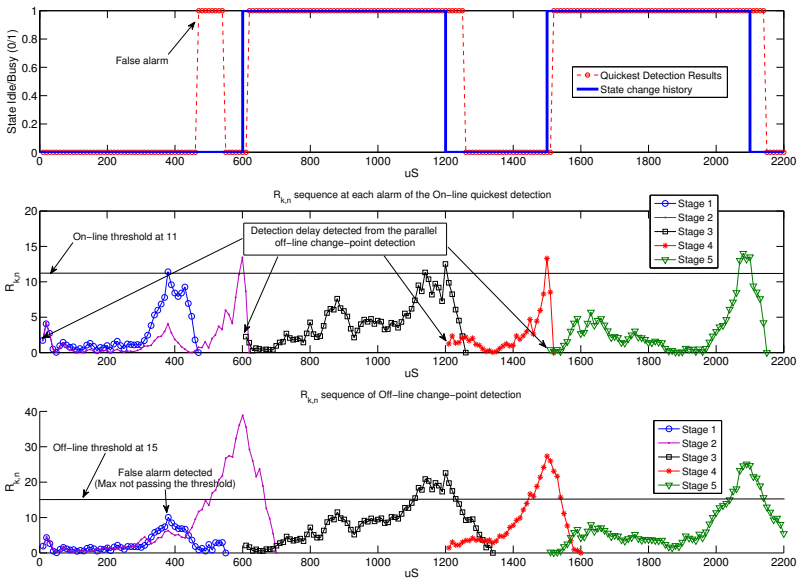

Fig. 3. A typical scenario of the multi-variate parallel on-line QD/offline change-point detection procedure at SNR$= -5$dB, with a sampling rate of 100MHz and sensing interval of 10μS.

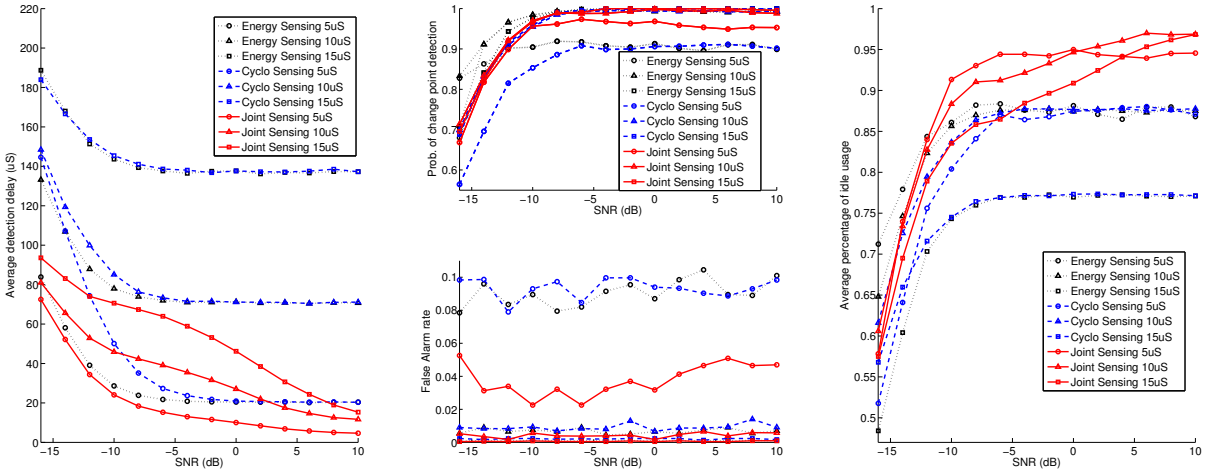

(a) Average detection delays.

(b) Probability of change-point detection and false alarm rate.

(c) Percentage of idle chanel usage.

Fig. 4. Performance comparisons of the average sample power-based, the cyclostationarity-based, and the multi-variate parallel QD strategies. With a sampling rate of 100MHz, the sensing time durations are set to 5μS, 10μS, and 15μS, respectively in all cases.

change-point detection and the false alarm probability are shown in Fig. 4(b), and the resulting percentage of idle state usage is shown in Fig. 4(c). In the two uni-variate QD cases, the threshold for the Shiryayev-Roberts statistic R_n was set to $A = 830$. In the multi-variate parallel QD case, the detection thresholds are set to be $h_{n,p_f} = 17$ and $h_{off} = 20$ in order to make the false alarm probabilities lower than the other two cases for a fair performance comparison. Note that higher threshold setting in all cases may result in lower false alarm probability but at the expense of less change-point detection and longer detection delays. The minimum idle/busy state sojourn time is set to 600μS in all three cases. For fair comparison, we assume that whenever a false alarm is raised prior to a state change from busy to idle, the following idle period is not used by the CR. However, in practice a CR may still make use of some portion of the idle period using the multi-variate parallel detection scheme. As we can see, slightly shorter detection delays are achieved by using the average sample power based QD, compared to that using the cyclostationarity-based features. However, by exploiting the power/cyclostationarity diversity, the multi-variate parallel QD scheme yields superior performance, in terms of both lower detection delays and lower false alarm probabilities for each sensing duration compared to the other two schemes. Although similar probabilities of change-point detections are achieved for all three schemes, the multi-variate parallel scheme yields much higher average percentage of idle channel usage in the SNR region from -10 to 10dB. It is also shown in Fig. 4(c) that the average sample power based scheme with sensing duration of 5uS achieves the highest average percentage of idle channel usage in SNR region from -16 to -12dB. This suggests that the average sample power based scheme may be more efficient in the extreme low SNR region compared to the other schemes.

From the performance comparisons shown in Fig. 4, we can also see the tradeoff between the length of sensing duration and the resulting percentage of usage of the idle state in all three cases. In particular, the highest percentage of usage is not necessarily always achieved by using the shortest sensing duration of 5μS, although it may achieve lower detection delays. This is due to its limited probability of change-point detection and comparatively high false alarm probability. Note that the false alarm probability is related to the ARL to false alarm. In particular, a shorter ARL to false alarm results in a higher false alarm probability. Moreover, the lower-bound of ARL to false alarm in (10) is given in terms of number of steps, but not in terms of the absolute time length. As a result, when using a shorter sensing duration for each step (with the same threshold value), false alarms are raised more frequently since there are more sensing steps prior to any change-point compared to that using a longer sensing duration for each step. This also points out the disadvantage of performing QD using individual samples (for example, the traditional individual sample power-based QD scheme proposed in [10]), which can be considered as the extreme case of using a short sensing duration.

The optimal setting of the sensing duration and the test threshold may not be easy to be derived analytically (since they depends on the pre and post-change distributions of the observations, which are assumed unknown in the first place). However, suitable machine learning (adaptive) techniques [26] may help in practice to find the optimal or a near-optimal solution. In particular, by using the proposed parallel on-line QD/off-line change-point detection scheme, performance feedback of detection delay and false alarm probability may help to estimate/predict the idle channel usage for any particular

setting. Then, an appropriately chosen machine learning algorithm may be used to find the optimal/near optimal solution.

V. Conclusions

In this paper, we proposed non-parametric quickest detection schemes to keep track of the state changes (idle/busy) of communication channels. This capability can be useful for future cognitive radios, since prior information on the statistics of channel usage is generally hard to obtain in practice. We also proposed a novel average sample power and cyclostationarity-based multi-variate parallel quickest detection/offline change-point detection scheme to improve detection performance compared to the traditional energy-based methods. The performance of the proposed detection schemes is evaluated through simulations. Compared to traditional energy-based quickest detection schemes, smaller detection delays and higher percentage of spectrum usage are obtained using the schemes proposed in this paper. The incorporation of the decision-making for wide-band spectrum sensing scheduling, and the evaluation of communication throughput are left as future work.

References

[1] "IEEE-USA President Commends FCC for National Broadband Plan [IEEE;USA]," *IEEE Antennas and Propagation Magazine*, vol. 52, no. 2, p. 179, April 2010.

[2] S. K. Jayaweera and C. G. Christodoulou, "Radiobots: Architecture, algorithms and realtime reconfigurable antenna designs for autonomous, self-learning future cognitive radios," University of New Mexico, Technical Report EECE-TR-11-0001, Mar. 2011. [Online]. Available: http://repository.unm.edu/handle/1928/12306

[3] M. Bkassiny, S. K. Jayaweera, Y. Li, and K. A. Avery, "Wideband spectrum sensing and non-parametric signal classification for autonomous self-learning cognitive radios," *IEEE Transactions on Wireless Communications*, pp. 2596 – 2605, Aug. 2011.

[4] S. Jayaweera, Y. Li, M. Bkassiny, C. Christodoulou, and K. Avery, "Radiobots: The autonomous, self-learning future cognitive radios," in *2011 International Symposium on Intelligent Signal Processing and Communications Systems (ISPACS), Chiang Mai, Thailand*, Dec. 2011, pp. 1 –5.

[5] C. Christodoulou, Y. Tawk, and S. Jayaweera, "Cognitive radio, reconfigurable antennas, and Radiobots," in *2012 IEEE International Workshop on Antenna Technology (iWAT), Tucson, Arizona, USA*, March 2012, pp. 16 –19.

[6] Y. Li, S. Jayaweera, and C. Christodoulou, "Wideband PHY/MAC bandwidth aggregation optimization for cognitive radios," in *2012 3rd International Workshop on Cognitive Information Processing (CIP), Parador de Baiona, Spain*, May 2012, pp. 1 – 6.

[7] M. Bkassiny, S. K. Jayaweera, Y. Li, and K. A. Avery, "Blind cyclostationary feature detection based spectrum sensing for Autonomous self-learning cognitive radios," in *IEEE International Conference on Communications (ICC '12), Ottawa, Canada,*, June 2012.

[8] Y. Li, S. Jayaweera, M. Bkassiny, and K. Avery, "Optimal myopic sensing and dynamic spectrum access in cognitive radio networks with low-complexity implementations," *IEEE Transactions on Wireless Communications*, vol. 11, no. 7, pp. 2412 –2423, July 2012.

[9] H. V. Poor and O. Hadjiliadis, *Quickest Detection*. Cambridge University Press, 2008. [Online]. Available: http://dx.doi.org/10.1017/CBO9780511754678

[10] L. Lai, Y. Fan, and H. Poor, "Quickest detection in cognitive radio: A sequential change detection framework," in *2008 IEEE Global Telecommunications Conference (GLOBECOM), New Orleans, Louisiana, USA*, Dec. 2008, pp. 1 –5.

[11] M. D. Holland, "A nonparametric change point model for multivariate phase-II statistical process control," Ph.D. dissertation, 2011.

[12] M. Duarte and A. Sabharwal, "Full-duplex wireless communications using off-the-shelf radios: Feasibility and first results," in *2010 Conference Record of the Forty Fourth Asilomar Conference on Signals, Systems and Computers (ASILOMAR), Monterey, California, USA*, Nov. 2010, pp. 1558 –1562.

[13] J. I. Choi, M. Jain, K. Srinivasan, P. Levis, and S. Katti, "Achieving single channel, full duplex wireless communication," in *Proceedings of the sixteenth annual international conference on Mobile computing and networking*, ser. MobiCom '10. New York, NY, USA: ACM, 2010, pp. 1–12. [Online]. Available: http://doi.acm.org/10.1145/1859995.1859997

[14] M. Jain, J. I. Choi, T. Kim, D. Bharadia, S. Seth, K. Srinivasan, P. Levis, S. Katti, and P. Sinha, "Practical, real-time, full duplex wireless," in *The 17th Annual International Conference on Mobile Computing and Networking (MOBICOM), Las Vegas, Nevada, USA*, 2011, pp. 301–312.

[15] M. Knox, "Single antenna full duplex communications using a common carrier," in *2012 IEEE 13th Annual Wireless and Microwave Technology Conference (WAMICON), Cocoa Beach, FL, USA*, April 2012, pp. 1 –6.

[16] S. Geirhofer, L. Tong, and B. Sadler, "A Measurement-Based Model for Dynamic Spectrum Access in WLAN Channels," in *2006 IEEE Military Communications Conference, 2006 (MILCOM)*, oct. 2006, pp. 1 –7.

[17] E. S. Page, "Continuous Inspection Schemes," *Biometrika*, vol. 41, no. 1/2, pp. 100–115, 1954. [Online]. Available: http://dx.doi.org/10.2307/2333009

[18] L. Gordon and M. Pollak, "A robust surveillance scheme for stochastically ordered alternatives," *Annals of Statistics*, vol. 23, pp. 1350 – 1375, Aug. 1995.

[19] W. Gardner, "Measurement of spectral correlation," *IEEE Transactions on Acoustics, Speech and Signal Processing*, vol. 34, no. 5, pp. 1111 – 1123, Oct. 1986.

[20] J. Parsons and A. Bajwa, "Wideband characterisation of fading mobile radio channels," *Communications, Radar and Signal Processing, IEE Proceedings F*, vol. 129, no. 2, p. 95, April 1982.

[21] M. Patzold, *Mobile Fading Channels*, 1st ed. John Wiley & Sons, Ltd, 2002.

[22] D.-S. Yoo and W. Stark, "Characterization of WSSUS channels: Normalized mean square covariance," *IEEE Transactions on Wireless Communications*, vol. 4, no. 4, pp. 1575 – 1584, July 2005.

[23] P. Hoeher, "A statistical discrete-time model for the WSSUS multipath channel," *IEEE Transactions on Vehicular Technology*, vol. 41, no. 4, pp. 461 –468, Nov. 1992.

[24] K.-W. Yip and T.-S. Ng, "Discrete-time model for digital communications over a frequency-selective Rician fading WSSUS channel," *Communications, IEE Proceedings-*, vol. 143, no. 1, pp. 37 –42, Feb. 1996.

[25] K. Choi and J. Marden, "An approach to multivariate rank tests in multivariate analysis of variance," *Journal of the American Statistical Association*, vol. 92, no. 440, pp. pp. 1581–1590, 1997. [Online]. Available: http://www.jstor.org/stable/2965429

[26] M. Bkassiny, Y. Li, and S. Jayaweera, "A Survey on Machine-Learning Techniques in Cognitive Radios," *IEEE Communications Surveys Tutorials,*, vol. PP, no. 99, pp. 1 –24, 2012.

Yang Li received the B.E. degree in Electrical Engineering from the Beijing University of Aeronautics and Astronautics, Beijing, China, in 2005 and the M.S. degree in Electrical Engineering from New Mexico Institute of Mining and Technology, Socorro, New Mexico, USA in 2009. He is currently working towards the PhD degree in Electrical Engineering at the Communication and Information Sciences Laboratory (CISL), Department of Electrical and Computer Engineering at the University of New Mexico, Albuquerque, NM, USA. His current research interests are in cognitive radios, spectrum sensing, cooperative communications, and dynamic spectrum access.

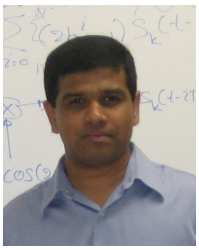

Sudharman K. Jayaweera (S00, M04, SM09) received the B.E. degree in Electrical and Electronic Engineering with First Class Honors from the University of Melbourne, Australia, in 1997 and M.A. and PhD degrees in Electrical Engineering from Princeton University in 2001 and 2003, respectively. He is currently an Associate Professor in Electrical Engineering at the Department of Electrical and Computer Engineering at University of New Mexico, Albuquerque, NM. Dr. Jayaweera is currently an associate editor of IEEE Transactions in Vehicular Technology. His current research interests include cooperative and cognitive communications, information theory of networked control systems, statistical signal processing and wireless communications.